Cell

EXTENDED EXPERIMENTAL PROCEDURES

Cell Culture Media

MCF10A full growth media consisted of phenol red-free DMEM/F12 supplemented with 5% horse serum, 20,000 pg/ml EGF, 10 μg/ml insulin, 0.5 μg/ml hydrocortisone, 100 ng/ml cholera toxin, 50 U/ml penicillin, and 50 μg/ml streptomycin. MCF10A starvation media ("GM-GFS") consisted of DMEM/F12 supplemented with 0.3% BSA, 0.5 μg/ml hydrocortisone, 100 ng/ml cholera toxin, and 50 U/ml penicillin, and 50 μg/ml streptomycin (Figures 2C–2E, and S4A). For experiments where mitogens were withdrawn, cells were washed three times with plain DMEM/F12 and placed in DMEM/F12 with penicillin/streptomycin (Figures 6B, 6C and 6E).

Constructs

To make the DHFR-Chy-p21 construct, p21 was amplified from cDNA containing a Tyr to Cys variant at amino acid 117. This variant is a documented SNP (#rs148679597) in NCBI's dbSNP database. We obtained the same results when we repeated the experiments in Figure 5C with Tyrosine at position 117, although we note that the steady state level was slightly higher.

Time-Lapse Microscopy

Cells were plated > 24 hr prior to imaging in full growth media in a 96-well dish (Costar #3904) at a density such that the cells remained sub-confluent even at the end of the imaging period. Time lapse imaging was performed in 290 μl full growth media, except in Figures 1F, 1G, 3C, 4A, 4B, 5C, and 6D where cells were imaged in 150 μl media until addition of a 2x spike of drug in 150ul media. Images were taken in CFP, YFP, RFP channels (depending on the experiment) every 12 min on an ImagExpress5000A microscope or an IXMicro microscope (Molecular Devices) with a 10X or 20X objective. Total light exposure time was kept under 525 ms for each time point. Cells were imaged in a humidified, 37°C chamber at 5% CO_2.

Image Processing

A low-pass Gaussian filter was first applied to each image. The local background value of each pixel was then determined by searching for a surrounding ring area, with the outer and inner radii of the ring being 10 and 5 times the approximate nuclear radius, respectively. The lowest 5th percentile value of the ring area was used as the background intensity of the center pixel. Cell nuclei were identified using fluorescent H2B images as masks. The MATLAB function *regionprops* was then used to label each nucleus and to retrieve the xy coordinates of all pixels in specific nuclei.

The level of immunofluorescence staining and of Cer-Cdt1 in each cell was calculated as the average value of the intensities from each pixel of the specific nucleus. The nuclear and cytoplasmic intensities of DHB-Ven were calculated by the average value of the intensities from pixels of the nuclear and cytoplasmic masks, respectively. The nuclear mask was determined from the H2B image described above. The cytoplasmic mask consisted of a ring around the nucleus. To avoid the inclusion of nuclear pixels in the calculation of the cytoplasmic signal, we used the area between two rings, an outer rim 2 μm from the nuclear mask and an inner rim 0.5 μm outside the nuclear mask (for images taken with the 20X objective). For images taken with the 10X objective, the outer and inner rims of the rings were 4 μm and 2 μm outside the nuclear mask, respectively. Because the shapes of the cells were irregular, the ring area may also cover some extracellular space. To avoid including background pixels in the calculation of the cytoplasmic DHB-Ven signal, we only averaged the pixels in the top 50th percentile.

To determine the time-lapse changes of Cer-Cdt1 and DHB-Ven signals, cell nuclei were tracked between time points. Because the stage jittered slightly after addition of drugs, after washing away mitogens, or after fixation and immunofluorescence, the H2B images between time frames were aligned before cell tracking was performed. We first subtracted the image at a specific time from the image in the next frame, to get a "difference score" between two images. We then repeated the process, with one image moving in a two-dimensional manner, to get multiple "difference scores" when the stage jittered. The position with the lowest score indicated the amount of jittering and the images were aligned and cropped accordingly.

Cell tracking was performed using a regional nearest neighborhood method. Briefly, each nucleus in a specific frame was linked to the nearest nucleus in the next time frame. Erroneous links were eliminated if the sizes or the shapes of the linked nuclei were dissimilar to each other, or if the distance between the nuclei went far beyond the distance that the cells could migrate between two time frames. A mitosis event (anaphase) was identified if two nuclei in a frame were of similar size and H2B intensity and if these two nuclei were linked to the same nucleus in the previous frame. Because the chromosomes were labeled by fluorescent H2B even after the breakdown of the nuclear envelope, the "nuclear" and "cytoplasmic" level of DHB-Ven could still be calculated during mitosis.

In Vitro Kinase Assays

ProQinase GmbH performed the purification of DHB and the in vitro kinase assays. Amino acids 994-1087 of DHB protein were cloned in-frame to the GST of plasmid pGEX3C3 under the control of the IPTG inducible T7 promoter. The plasmid was amplified by transformation in chemically competent *E.coli* (DH5α) and purified by DNA midiprep. Chemically competent *E. coli* BL21 bacteria were transformed with midi prep DNA of the plasmid and selected using ampicillin. Overnight cultures of the recombinant bacteria were used to inoculate productive cultures, grown to an appropriate optical density, and induced by addition of IPTG. Bacteria were cultivated for another 3 or 6 hr after induction, harvested by centrifugation and the pellets were frozen at −80°C. Purification of the recombinant protein was done by GST-GSH affinity chromatography, with the final elution/storage buffer containing 50 mM HEPES

pH 7.5, 100 mM NaCl, 1 mM DTT, 15 mM reduced glutathione, and 10% glycerol. Protein concentration was determined to be 550 μg/ml using the Bradford method with BSA (Sigma, cat# A-7638, Lot 79H7641) as standard protein. Protein purity was assessed by means of a coomassie-stained SDS-PAGE of different amounts of protein.

An established positive control, the generic cyclin-CDK substrate GST-RBER-CHKtide, was expressed in *E.coli* BL21 and purified by means of GST-GSH affinity chromatography followed by ion-exchange chromatography. Buffer conditions and determination of protein concentration (1100 μg/ml) were identical to those described for DHB. All protein kinases provided by ProQinase were expressed in Sf9 insect cells as recombinant GST-fusion proteins or His-tagged proteins. All kinases were produced from human cDNAs. Kinases were purified by either GSH-affinity chromatography or immobilized-metal affinity chromatography. The purity of the protein kinases was examined by SDS-PAGE/Coomassie staining, and the identity was checked by mass spectroscopy.

A radiometric protein kinase assay (33PanQinase Activity Assay) was used for measuring the kinase activity of the 5 protein kinases. All kinase assays were performed in 96-well FlashPlates from PerkinElmer (Boston, MA) in a 50 μl reaction volume. The reaction cocktail was pipetted in four steps in the following order: 10 μl of ATP solution (in H_2O), 20 μl of assay buffer + ^{33}P-γ-ATP, 10 μl of substrate, and 10 μl of enzyme solution.

The assay contained 70 mM HEPES-NaOH pH 7.5, 3 mM $MgCl_2$, 3 mM $MnCl_2$, 3 μM Na-orthovanadate, 1.2 mM DTT, ATP (variable amounts, corresponding to the apparent ATP-K_m of the respective kinase), [γ-^{33}P]-ATP (approx. 8×10^5 cpm per well), protein kinase (variable amounts), and substrate (variable amounts). See Table S1 for details. The reaction cocktails were incubated at 30°C for 60 min. The reaction was stopped with 50 μl of 2% (v/v) H_3PO_4, and plates were aspirated and washed two times with 200 μl 0.9% (w/v) NaCl. Incorporation of $^{33}P_i$ was determined with a microplate scintillation counter (Microbeta, Wallac).

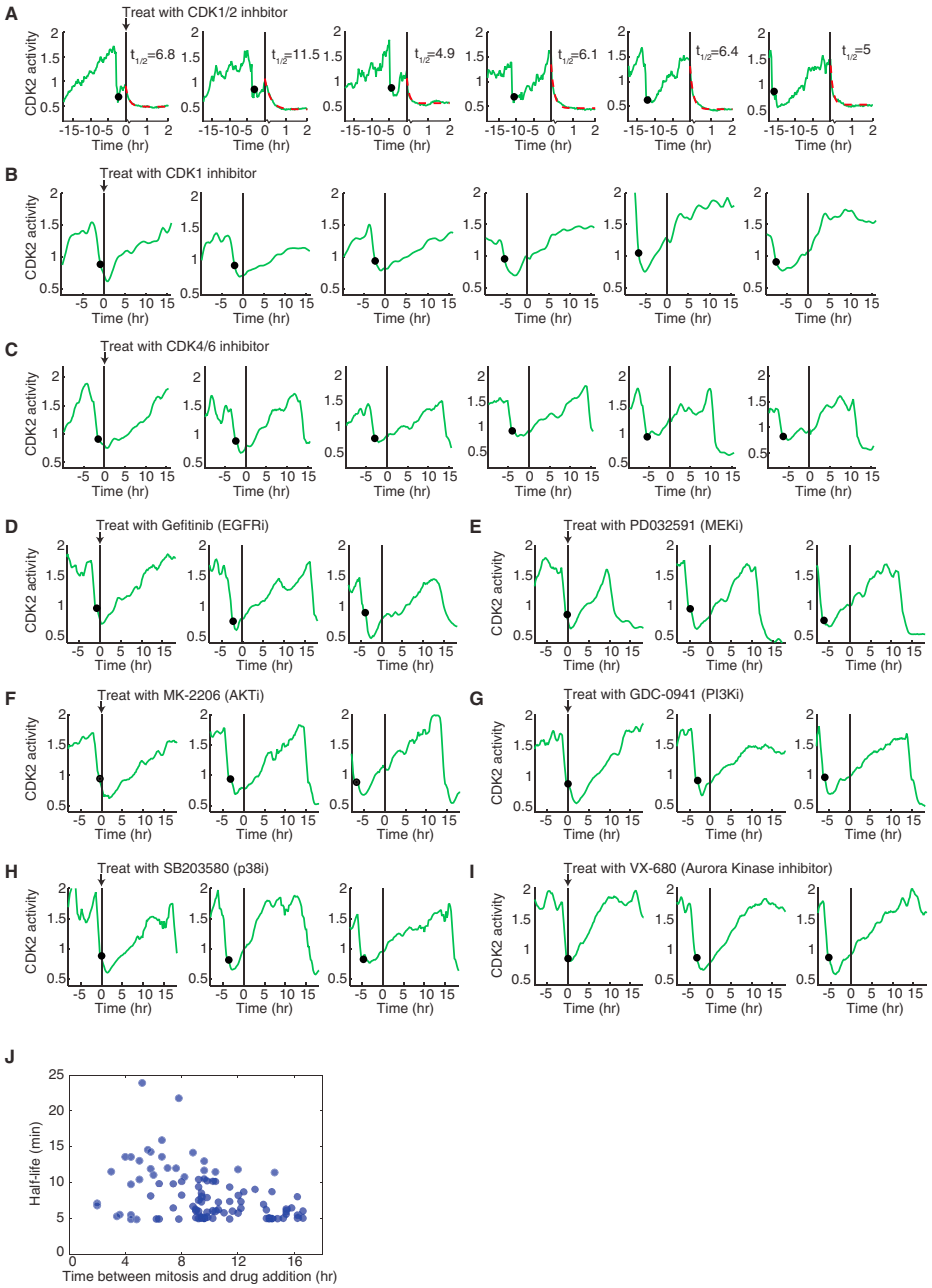

Figure S1. DHB-Ven Localization Is Affected by a CDK1/2 Inhibitor but Not by a Variety of Other Kinase Inhibitors, Related to Figure 1

(A) Cyt/Nuc DHB-Ven traces in individual MCF10A cells before (imaged every 12 min) and after (imaged every 2 min) treatment with 10 μM CDK1/2i (EMD Biosciences #217714) at t = 0 hr (marked by vertical black line). Cells are plotted in order of increasing time between mitosis (black dot) and drug treatment. Only $CDK2^{inc}$ cells were used because the drug has no effect on translocation of the sensor in $CDK2^{low}$ cells because the sensor is already maximally nuclear (see Figures 4A and 4B). The half-life of retro-translocation of the sensor from the cytoplasm to the nucleus was calculated by fitting each trajectory to an exponential decay (red dashed line). The fitted half-life (in minutes) for each cell is marked in each plot.

(B-I) Individual cells were treated with the indicated drug at t = 0 hr (marked by vertical line). Cells are plotted in order of increasing time between mitosis (black dot) and drug treatment. Images were taken every 12 min. B) 9 μM CDK1 inhibitor (RO-3306), C) 1 μM CDK4/6 inhibitor (PD0332991), D) 10 μM EGFR inhibitor (Gefitinib), E) 100 nM MEK inhibitor (PD032591), F) 1 μM AKT inhibitor (MK-2206), G) 1 μM PI3K inhibitor (GDC-0941), H) 10 μM p38 inhibitor (SB203580), I) 3 μM Aurora Kinase inhibitor (VX-680).

(J) Data from the experiment in (A) (n = 99 cells). The mean of individual fits is 8.2 min and the standard deviation is 3.6 min. Given the frame rate, half-lives much below 5 min cannot be properly resolved. The fact that the half-life is relatively constant through interphase implies that the phosphatase activity acting on the sensor is constant and that the observed translocation of the sensor from the nucleus to the cytoplasm can be interpreted as relative kinase activity.

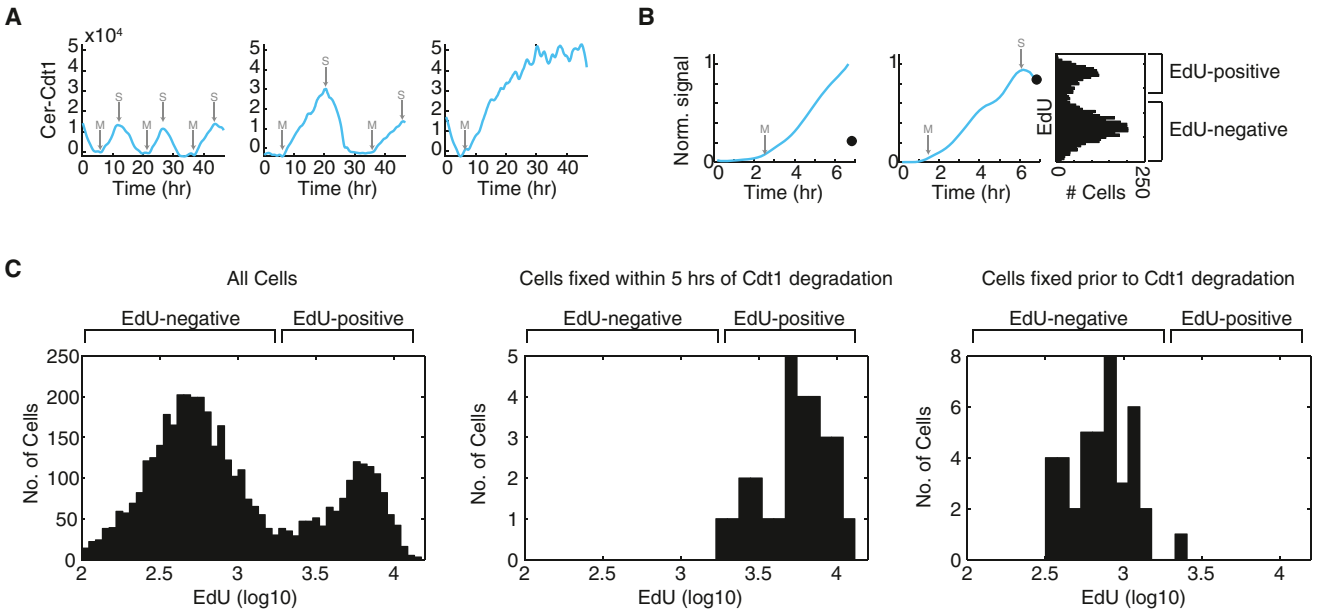

Figure S2. S Phase Begins Once Cdt1 Degradation Has Been Induced, Related to Figure 2

(A) Representative single-cell traces of Cer-Cdt1. Cer-Cdt1 increases during G1 and is degraded by the SCF^{Skp2} E3 ligase at the start of S phase. The levels of Cer-Cdt1 are regulated only by proteolysis and thus Cer-Cdt1intensity is proportional to the elapsed time between M and the activation of SCF^{Skp2} at the start of S. Left, a cell with M-to-S intervals of 5-7 hr. Middle, a cell with an M-to-S interval of 14 hr. Right, a cell with an M-to-S interval of > 40 hr.

(B) Time-lapse imaging of Cerulean-Cdt1 was followed immediately by addition of 10 μM EdU for 15 min, fixation, and visualization of the EdU signal. The image of the EdU signal was precisely aligned to the time-lapse movie using a custom jitter correction algorithm. This enabled matching of the Cdt1 trace of each cell to its EdU signal at the end of the movie. Images were taken every 10 min. Example showing the Cer-Cdt1 trace and EdU intensity in two MCF10A cells. Left, Single-cell Cer-Cdt1 trace (blue) in which the degradation of Cer-Cdt1 had not yet begun before the end of the imaging period. Correspondingly, the cell did not incorporate EdU (black dot). Middle, Single-cell Cer-Cdt1 trace (blue) in which the degradation of Cer-Cdt1 was initiated, marking the start of S phase. Correspondingly, the cell is EdU-positive (black dot). Right, Histogram, log scale, of EdU intensities in all cells in the population, used to establish the boundary between EdU-negative and EdU-positive cells. The black dots in the left and middle panels can be directly mapped onto this histogram.

(C) Left, Histogram, log scale, of EdU signal in all MCF10A cells in the population, regardless of cell-cycle phase, used to establish the boundary between EdU-negative and EdU-positive cells. Cells in left side of distribution are EdU negative and not in S phase; cells in the right side of the distribution are EdU positive and in S phase. Middle, Histogram of EdU signal in cells that were fixed within 5 hr of induction of Cdt1 degradation; these cells are EdU positive. Right, Histogram of EdU signal in cells that had a mitosis but Cdt1 degradation had not yet occurred at the time of fixation; these cells are EdU negative.

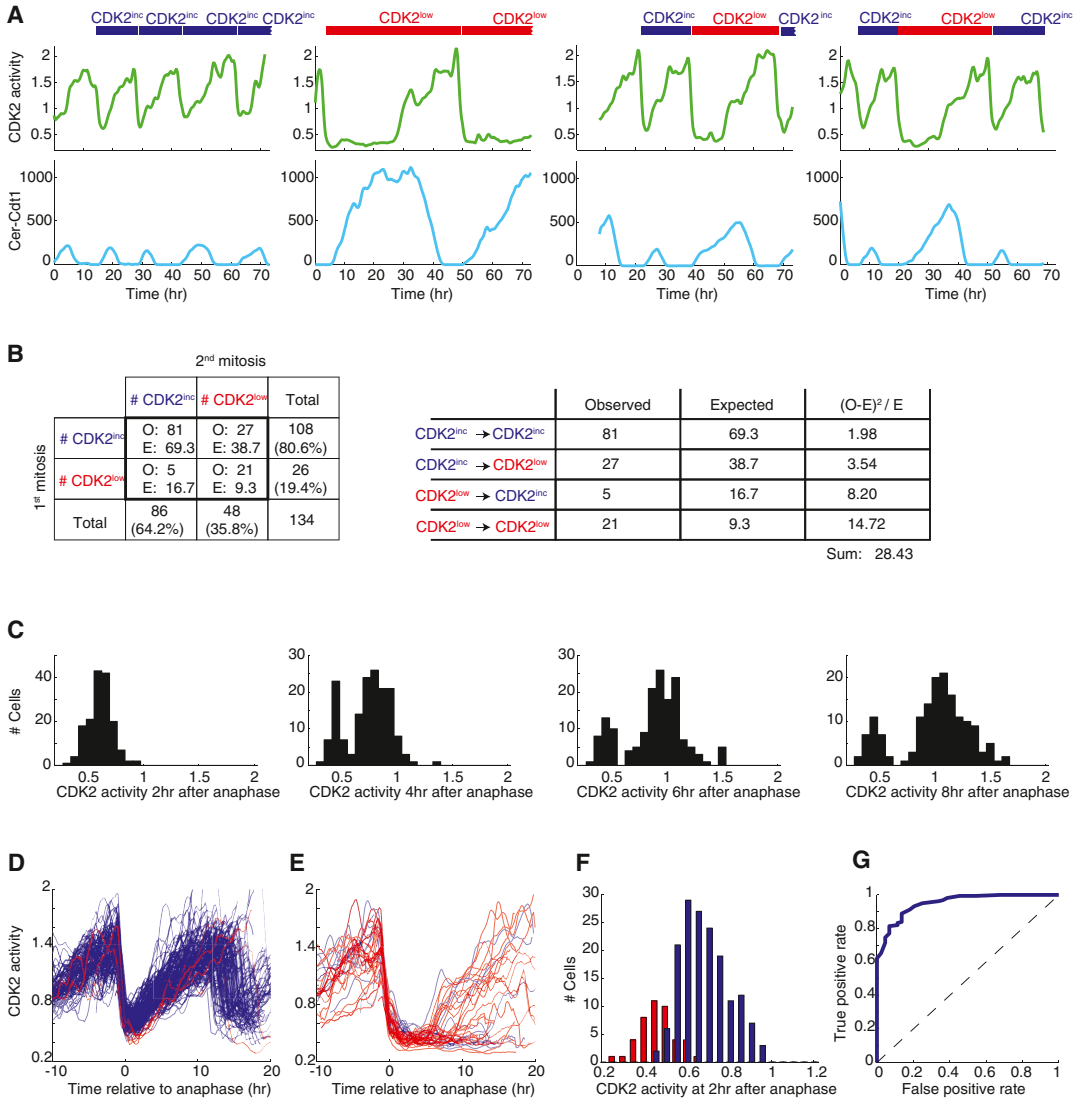

Figure S3. Additional Characterization of the Bifurcation in CDK2 Activity, Related to Figure 3

(A) Four cells demonstrating transitions at mitosis from CDK2^{inc} to CDK2^{inc}, CDK2^{low} to CDK2^{low}, CDK2^{inc} to CDK2^{low} and CDK2^{low} to CDK2^{inc}. The fact that a CDK2^{low} cell can convert into a CDK2^{inc} cell shows that the CDK2^{low} cells are not simply sick or unhealthy. Top, CDK2 activity over time, measured by DHB-Ven. Bottom, Cer-Cdt1 intensity over time. Colored bars mark the length of one cell cycle.

(B) Table showing the number of cells entering the CDK2^{inc} or CDK2^{low} state after a 2nd mitosis given that they entered the CDK2^{inc} or CDK2^{low} state after a 1st mitosis. Using the null hypothesis that each mitosis is independent, we obtain a Chi^2 value of 28.43, and reject the null hypothesis with $p << 0.001$. Thus, CDK2^{inc} and CDK2^{low} cells can interconvert, but the CDK2^{inc} versus CDK2^{low} decision is not independent of previous decisions.

(C) Distribution of CDK2 activity at 2hr, 4hr, 6hr or 8hr after anaphase, for bifurcating MCF10A cells as in Figure 3B. The continuous distribution of CDK2 activity at 2hr after anaphase evolves into a bimodal distribution by 4hr after anaphase, indicating two discrete populations.

(D-E) MCF10A DHB-Ven traces separated manually into CDK2^{inc} cells (D) and CDK2^{low} cells (E). Traces were colored red if the Cyt/Nuc ratio of DHB-Ven fell below a cutoff of 0.55 at 2hr after anaphase; otherwise the traces were colored blue. Using this coloring scheme, 6/160 cells were mis-colored red in (D) and 15/44 cells were mis-colored blue in (E). In total, the future behavior of 183/204 (90%) of cells was correctly classified based on the DHB-Ven signal at 2hr after anaphase.

(F) CDK2 activity at 2hr after anaphase for CDK2^{inc} cells (blue) and CDK2^{low} cells (red). The point of intersection between the two distributions is close to DHB-Ven = 0.55 and gives the best separation between the two behaviors.

(G) Receiver Operating Characteristic (ROC) curve for cells in (D) and (E) as the cutoff is varied from 0.23 to 0.98. "True positives" are cells in (D) that were correctly colored blue; "false positives" are cells in (E) that were incorrectly colored blue. At a cutoff of 0.43, we capture 100% of the true positives, but have a false positive rate of 68%. At a cutoff of 0.5, have a true positive rate of 96% and a false positive rate of 34%. At a cutoff of 0.63, we have a true positive rate of 62% but have zero false positives. Thus, DHB-Ven $\leq$ 0.43 at 2hr after anaphase is 100% predictive of entry into the CDK2^{low} state, whereas DHB-Ven $\geq$ 0.63 is 100% predictive of an immediate entry into the next cell cycle.

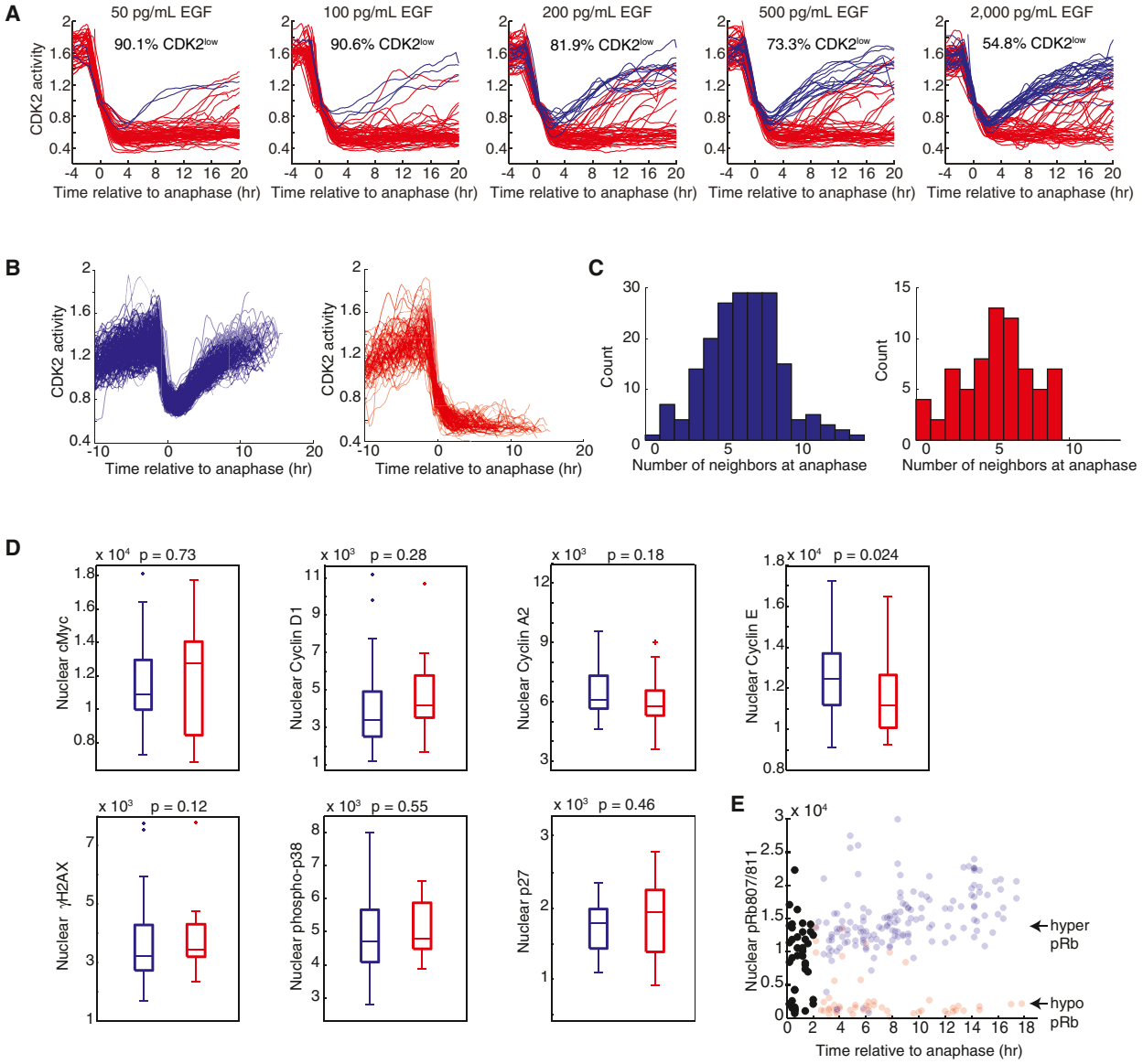

Figure S4. Entry into the CDK2^{low} State Is Not Correlated with Local Cell Density or with Differences in the Levels/Phosphorylation States of Several Other Proteins, Related to Figure 4

(A) MCF10A cells were starved for 24hrs in GM-GFS media and then supplemented with the indicated concentration of EGF. Imaging was started 8hrs after stimulation with EGF.

(B) CDK2^{inc} cells that did not undergo a second mitosis (blue) and CDK2^{low} cells that remained in the CDK2^{low} state (red) were selected for analysis in (C)–(E).

(C) Number of neighbors surrounding a given cell at anaphase, for cells in (B). Any cell nucleus within a 100 pixel (50 micron) radius at the time of anaphase was counted as a neighbor of the cell of interest. Athough these cells do undergo contact inhibition at very high densities (at which time DHB-Ven does localize to the nucleus), there is no evidence for contact inhibition sending the cells into the CDK2^{low} state at the subconfluent densities used in our time-lapse imaging experiments.

(D) At the end of the imaging period, cells were immediately fixed with formaldehyde, permeabilized, and stained with various antibodies. The antibody stain in each cell was matched back to the cell's history as described in Figure 4. CDK2^{inc} (blue) and CDK2^{low} (red) cells that had undergone anaphase 2-3.5hr prior to fixation were selected for comparison in the boxplots. A Rank Sum statistical test was used to obtain p values. The following antibodies were used: cMyc (Cell Signaling Technology #5605), cyclin D1 (Neomarkers #RM-9104-S1), cyclin E (Invitrogen #32-1600), cyclin A2 (Santa Cruz Biotechnology #sc-751), γH2AX (Millipore #05-636), phospho-p38 (Cell Signaling Technology #4511), p27 (BD 610241).

(E) Time-lapse imaging of CDK2 activity in asynchronous cells was followed by immunofluorescence staining for pRb807/811, as described in Figure 4C. Black dots mark pRb807/811 levels in cells before the bifurcation in CDK2 activity was apparent and show that two sub-populations of phospho-Rb are evident even within the first hour after anaphase. Faded blue and red dots are reproduced from Figure 4E.

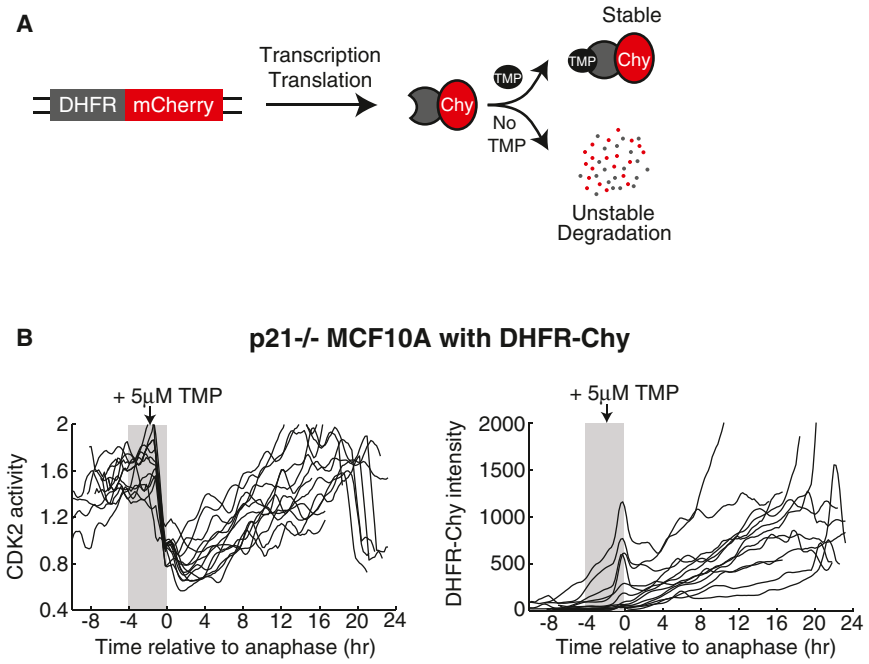

Figure S5. DHFR-mCherry Expression Is Induced by TMP Treatment which Does Not Affect Normal Cell-Cycle Progression, Related to Figure 5

(A) Schematic of DHFR-mCherry construct. Under basal conditions, DHFR-mCherry is unstable and is degraded. Upon addition of TMP, DHFR-mCherry is stabilized and accumulates in cells.

(B) p21$^{-/-}$ MCF10A cells were transduced with DHFR-Chy and selected with puromycin. Cells that received TMP in the 4 hr prior to mitosis (represented by gray bar) are shown. TMP addition and consequent mCherry accumulation had no effect on cell-cycle progression.

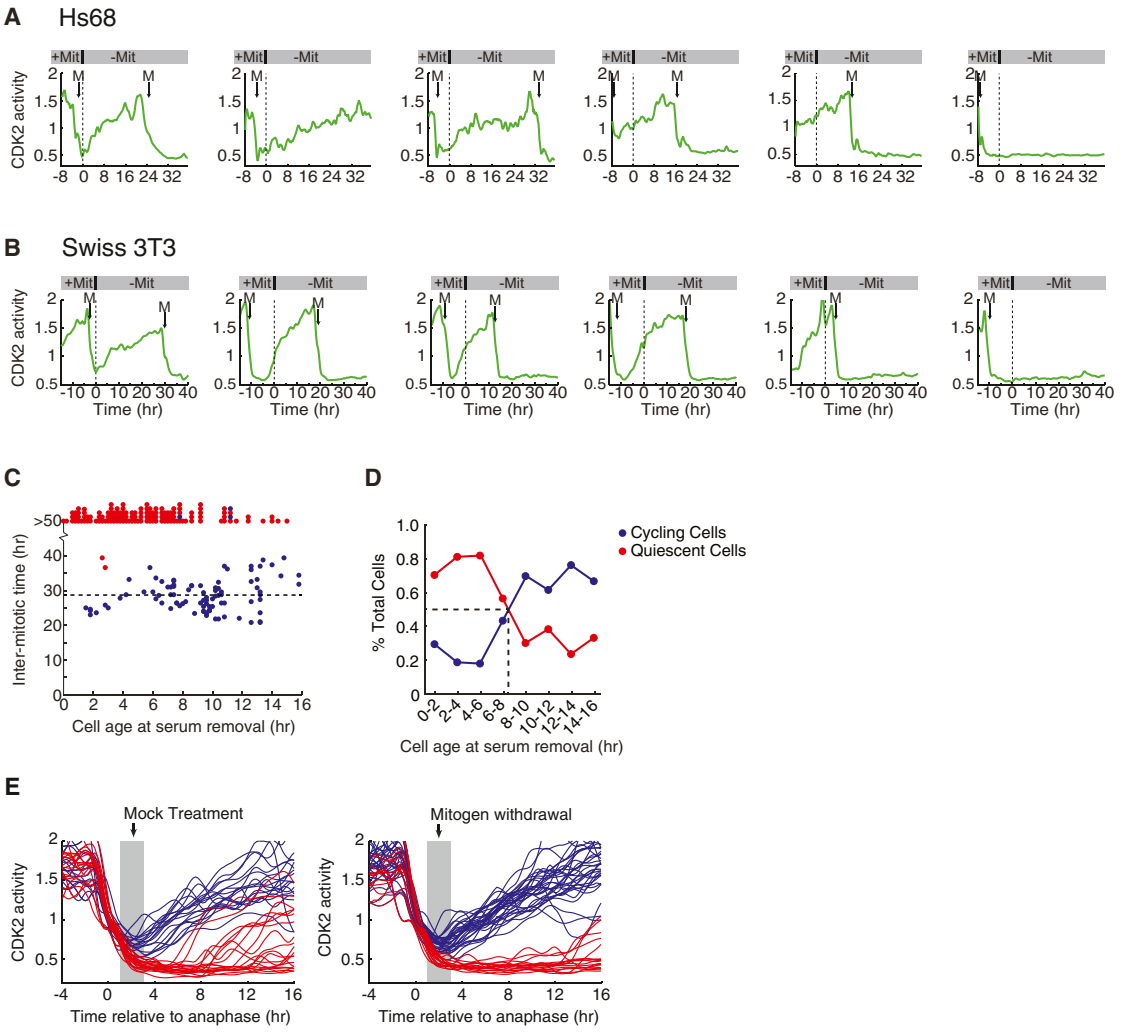

Figure S6. Serum Removal Increases the Probability of Entering Quiesence, Related to Figure 6

(A-B) Hs68 primary foreskin fibroblasts (A) or Swiss 3T3 cells were preimaged in full growth media, washed three times with DMEM, then transferred to serum-free DMEM (dashed line at t = 0). Once initiated, CDK2 activity continues to build up even when mitogens are removed.

(C) Data from the experiment described in (B), displayed as a scatter plot (reproduced from Figure 6G). For each cell, the time between the last mitosis and the time serum was removed was recorded (cell age at serum removal), as well as the length of the subsequent cell cycle (intermitotic time). Cells are colored red if CDK2 activity was not yet building up when mitogens were removed; these cells remain in the CDK2^{low} state. Cells are colored blue if CDK2 activity was already building up when mitogens were removed; these cells continue to build up CDK2 activity, complete mitosis, and then enter the CDK2^{low} state. The probability of entering quiescence (defined here as an intermitotic time of > 50 hr) decreases with an increase in cell age at serum removal, as it becomes more and more likely that cells will have entered a mitogen-insensitive state of increasing CDK2 activity. Images were taken every 12 min for a total of 66 hr. n = 229 cells. (Compare to Zetterberg and Larsson, 1985; Figure 1).

(D) Percentages of cycling versus quiescent cells were determined from (C). Cells with an intermitotic time of > 50 hr were designated quiescent. Cells were binned in 2 hr intervals. Dotted line denotes the time at which there is a 50% chance of becoming quiescent. Unlike Zetterberg and Larsson (1985), we did not find that CDK2^{low} cells have a sharp cutoff in susceptibility to serum withdrawal at 4 hr after anaphase as reported. Instead, we found a more gradual shift in the probability to re-enter the cell cycle as a larger and larger fraction of cells emerged from the CDK2^{low} state, built up CDK2 activity, and became again insensitive to serum withdrawal.

(E) MCF10A cells were preimaged for 8 hr in full growth media, washed three times, then transferred to full growth media (mock treatment) or to plain media without mitogens. Only cells that had completed anaphase 1-3 hr prior to mitogen removal are plotted. Mitogens were absent for the remainder of the imaging period. 45 cells are plotted in each panel.